Available online at www.sciencedirect.com
SCIENCE DIRECT
Polymer 46 (2005) 10952–10959
polymer
www.elsevier.com/locate/polymer

Morphology and photophysical properties of phenyleneethynylene oligomer

Chuan-Zhen Zhou, Tianxi Liu, Ting-Ting Lin, Xin-Hai Zhan, Zhi-Kuan Chen*

Institute of Materials Research and Engineering (IMRE), 3 Research Link, Singapore 117602, Singapore

Received 11 December 2004; received in revised form 16 August 2005; accepted 7 September 2005
Available online 26 September 2005

Abstract

The influence of annealing on the morphologies and optical properties of phenyleneethynylene pentamer films has been investigated by using optical microscopy, UV–vis spectroscopy, steady-state and time-resolved photoluminescence (PL). The optical microscopy study shows that the grainy morphology of crystallites with irregular shapes and sizes of the spincoated oligomer films reorganize into well-ordered single crystal-like laths or bamboo-like structures upon melt-crystallization or annealing. The crystalline features of the annealed films were simulated and modeled through molecular mechanics (MM) and molecular dynamics (MD) and further measured by X-ray diffraction. These studies revealed that the molecular backbones form lamellar and interdigitated conformations. Investigation of optical properties of the thermally treated films indicated that aggregates and excimers dominate excitation/emission processes due to molecular closely packing upon annealing, which are evidenced by the broadening, structureless absorption and luminescence spectra, as well as longer lifetime of PL dynamics.

Keywords: Oligo(phenyleneethynylene); Morphology; Photophysical property

1. Introduction

In recent years, much effort has been paid on the syntheses and studies of conjugated polymers and their oligomers due to their combined electronic and optical properties as semiconductors, solution processability and mechanical flexibility as plastics and wide potential applications in light-emitting devices (LEDs) [1,2], field-effect transistors (FETs) [3], photovoltaic and solar cells [4], lasers [5] and molecular scale electronics [6,7]. Generally, the performance of conjugated materials in all of these applications is mainly governed by the chemical structure of the active materials and the device architecture. However, other factors such as the processing conditions for film preparation, which are closely related to the film morphologies, play an even more important role in some cases. For instance, the field effect mobility of pentacene-based organic FETs in highly ordered morphology can be nine order of magnitudes greater than that in amorphous films [8]. In addition, improvement of quantum efficiencies in OLEDs or photovoltaic cells through the control of film morphologies to (i) decrease the amount of interchain interactions [9,10], (ii) optimize the charge carrier mobility [11,12], or (iii) enhance the exciton dissociation and photocurrent collection [13,14], has also been reported recently. The reason that device performance is strongly influenced by the film morphology is that the electronic properties of the conjugated polymer or oligomer molecules are directly and closely related to the inter/intra-chain interactions, which are determined by molecular alignment and the distance from each other. Therefore, better understanding of the relationship between the molecular packing/interaction and optical and electronic properties of the polymer films is essential for optimizing device performance [15,16]. The morphologies of the spincoated polymer films can be varied by changing the spin speed, the organic solvents used, and the concentration of the polymer solution [17,18]. Thermal annealing the polymer films can also be applied to modify their morphologies and to control the degree of interchain interactions [19]. The morphologies of annealed films can be significantly different from spincoated films. During the process of spincoating, the solvent is quickly evaporated so that the polymer chains are frozen in a random way and can form varieties of conformations. On the contrary, thermal annealing of the polymer films will provide the necessary energy to make the different conformations in the spincoated film converge to a similar morphology in which both the main chains and side chains of the polymers are packed in a more ordered fashion [20].

* Corresponding author. Fax: +65 6872 0785.
E-mail address: zk-chen@imre.a-star.edu.sg (Z.-K. Chen).

0032-3861/$ - see front matter © 2005 Elsevier Ltd. All rights reserved.
doi:10.1016/j.polymer.2005.09.030

Among the conjugated polymers, rigid-rod poly(*p*-phenyleneethynylene)s (PPEs) and their corresponding oligo(*p*-phenyleneethynylene)s (OPEs) are one of the most investigated materials because of their potential applications in polymer LEDs [21] and molecular electronics [7,22]. Much work on optical properties and solid state morphologies of alkyl- and alkoxy-substituted PPEs has been reported [23,24]. It has been shown that substituted PPEs exhibit either lamellar or interdigitated morphology in solid state, depending on the density of the side-chains attached. Aggregates and excimers have been identified in these polymer films through absorption and photoluminescence spectroscopy investigations [23,25]. However, little is known about the correlation between the morphology and optical properties of OPEs. Recently, we have developed a series of alkoxy substituted OPEs with different terminal groups and investigated their absorption and emission properties in solution and solid state. In addition, the self-organized crystalline morphology of trimethylsilyl (TMS)-terminated pentamer was studied [26]. In order to gain better understanding of the relationship between the microscopic organization and optical properties of OPEs in films, we examine the spincoated and thermally annealed films of TMS-terminated pentamer using a combination of different characterization methods. Optical microscopy (OM) and X-ray diffraction (XRD) were used to investigate the crystalline morphology and molecular packing. The optical spectra of the films were studied using steady-state and time-resolved photoluminescence. Additionally, theoretical modeling based on molecular mechanics/molecular dynamics (MM/MD) calculation has been performed to propose the molecular packing. The morphologies obtained from OM and XRD can be interpreted by simulation models of chain organization.

2. Experimental section

2.1. Materials

The oligo(*p*-phenyleneethynylene) pentamer with TMS-termini was prepared by a stepwise synthetic method [26]. The films were prepared by spincoating the oligomer/xylene solution (ca. 2% (w/v)) on quartz plates at ambient temperature. In order to investigate the effect of annealing on the optical properties and morphologies of the oligomer films, the films were heated to 160 °C (the melting point of the oligomer is 147 °C), held for 5 min, then cooled at 20 °C/min to 70 or 120 °C for annealing for 30 min (i.e. melt-crystallization). All the thermal treatments were performed in a differential scanning calorimeter (DSC-2920 from TA Instruments) under nitrogen atmosphere in order to diminish oxidation. The morphologies of the spincoated and annealed films were observed using an Olympus optical microscope.

2.2. Methods

The absorption and steady-state photoluminescent spectra were obtained using a Shimadzu UV-3101 PC UV–vis–NIR spectrophotometer and a Perkin–Elmer LS-50B luminescence spectrophotometer with a xenon lamp as light source, respectively. The samples for time-resolved photoluminescence measurements were excited by the frequency-doubled output of a Ti:sapphire femtosecond laser. The excitation pulses were centered at 400 nm with pulse duration of 200 fs and a repetition rate of 82 MHz. The PL was dispersed by a 0.25 m monochromator and recorded by a streak camera with a time resolution of 15 ps. X-ray diffraction patterns were measured using Bruker AXS diffractometer at 40 mA and 40 kV. Molecular mechanics (MM) and molecular dynamics (MD) simulations were carried out using Cerius^2 software package. COMPASS [27] force field was applied because it has parameters for both the TMS-terminated pentamer molecules and the substrate quartz crystal.

3. Results and discussion

Fig. 1(A) shows an optical micrograph for the spincoated film with a thickness of ~150 nm of the OPE pentamer. A homogeneous grainy morphology of numerous crystallites with irregular shapes and size of less than 10 μm is observed, indicating a substantially less ordered or imperfect structure. However, after keeping the sample at 160 °C for 5 min followed by quenching to room temperature, most grainy crystallites observed in the spincoated film reorganize into a number of crystalline strips (Fig. 1(B)). Interestingly, upon melt-crystallization or annealing at 70 °C for 30 min, numerous well-developed lamellar laths with dimensions of *ca*. tens of micrometers in length and a few micrometers in width are observed (Fig. 1(C)). These laths are slightly curved and have no preferential orientation. Clearly, heating the oligomer films above the melting point (147 °C) and then cooling to the designed temperature for annealing leads to remarkable growth of typical polymeric lamellae with higher degree of molecular ordering in the single-crystal-like laths.

These narrow micro-laths in the melt-annealed oligomer films can be extended to larger scale, which could favor an increase of the charge carrier mobility in electronic or optoelectronic applications. For instance, when the spincoated solid films of the pentamer prepared from highly diluted xylene solution (in this case, the film thickness is about 10–20 nm) were melt-crystallized at a higher temperature, e.g. 120 °C for 30 min, besides the general features mentioned above, a unique 'bamboo' crystalline morphology is always observed (Fig. 1(D)). These 'bamboos' with lengths of hundreds micrometers and lateral sizes of a few to tens micrometers are composed of many crystalline joints (as indicated by arrows), which are connected intimately with each other and are probably the building blocks or units of the bamboo structure. The phenyleneethynylene-based rigid cores of the oligomer may act as mesogenic architecture for the packing of such bamboo morphology. So far, we have not found closely related examples for this type of crystalline morphology in literature. At higher crystallization temperature (e.g. 120 °C), the number of nuclei is drastically reduced. In addition, the grain shape and orientation are governed by surface free energy. As a result, the crystallites can develop laterally along

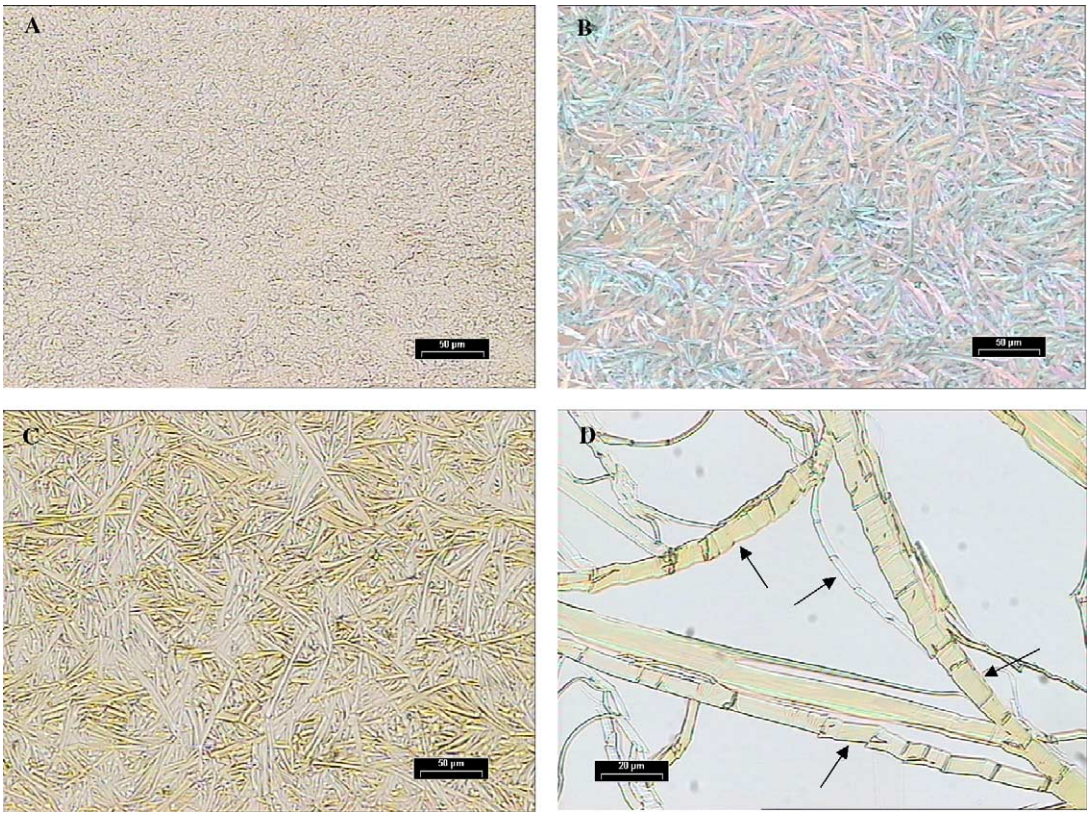

Fig. 1. Optical micrographs of OPE pentamer films spincoated (A), melt-quenched (B), annealed at 70 °C (C), and 120 °C (D).

one preferential growth axis, leading to the lamellar features observed. The lamellar laths and bamboo structures of the pentamer films are simulated and will be further discussed later on.

Annealing or melt-crystallization will change the conformations of the stiff backbone and the flexible side chains of the conjugated oligomers as well as their packing [28], which can be reflected in the change of the optical properties of the melt-grown films. Upon annealing, the less ordered grains reorganize into perfect single crystal-like lamellar laths or connected bamboo-like structures. The networks formed by such perfection and connection may lead to an improvement of the electric charge transport because the coupling or connection of the tightly packed molecules will lead to formation of delocalized excited states (excitons) through the coherent excitation of a number of conjugated molecules [29].

In order to better understand how changes in morphology of spincoated and annealed oligomer films affect their optical properties, UV–vis absorption, steady-state and time-resolved photoluminescence spectra of the dilute THF solution, spincoated and annealed films of OPE pentamer have been measured. The pentamer films used here are the same as those used in the morphological studies. The absorption and fluorescence spectra of dilute solution, spincoated and melt-crystallized films are shown in Fig. 2(A) and (B), respectively. The wavelengths of the absorption and emission peaks are summarized in Table 1. The dilute solution sample demonstrates single smooth absorption peak in the range of 350–460 nm. It is noted that the absorption spectra of the oligomer in solid states exhibit significant changes compared to that of the solution sample. There are three highly structured absorption peaks in UV spectra of the spincoated film, which are centered at 425, 437, and 461 nm. The well-resolved structure of the absorption spectra is ascribed to the ordered organization of the oligomer in solid state [30]. Melt-crystallization of the films at room temperature or annealing at 70 and 120 °C causes broadening of the absorption bandwidth and less fine-structured peaks. The absorption maxima of the three annealed films are around 436 and 465 nm. Additional obvious absorption tails in the range of 500–650 nm are observed for the three annealed film samples. The observed spectral broadening, red-shift of the main peaks as well as the existence of absorption tails in the low energy region of the thermally treated films, compared to the spincoated sample, strongly suggest the formation of aggregates in the films, caused by the close and ordered packing of the molecules after thermal treatment [31]. This behavior is in agreement with the highly ordered morphology observed in the optical micrographs of the annealed films and is further supported by the time-resolved photoluminescence measurements.

Photoluminescence spectroscopy is a useful tool for investigating molecular organization of conjugated materials because their spectra are sensitive to the aggregate and excimer species of the chromophores [32]. Fluorescence spectra of pentamer in solution, spincoated and annealed films have

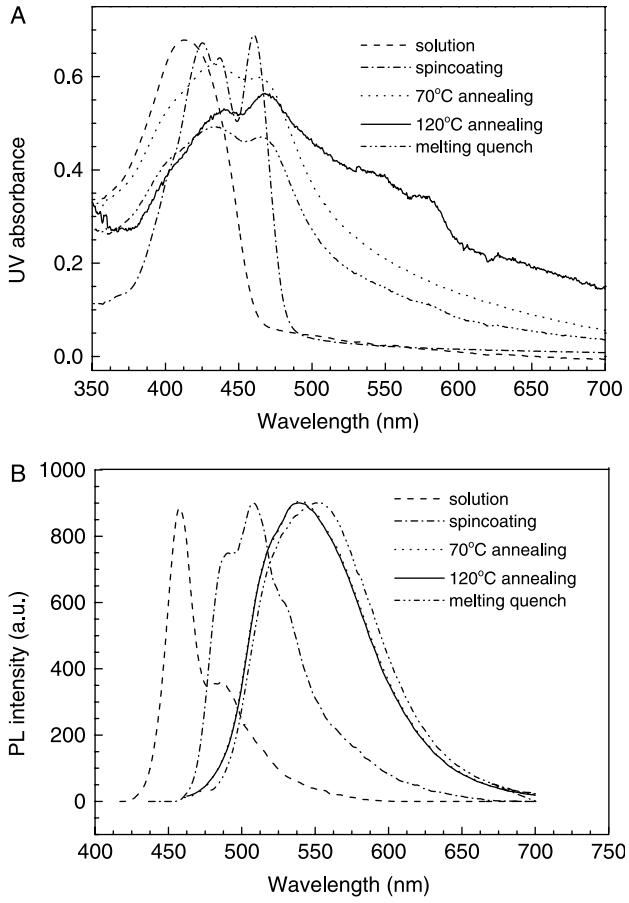

Fig. 2. UV–vis absorption (A) and photoluminescence (B) spectra of OPE pentamer in THF solution, spincoated film, annealed film at 70 °C, annealed film at 120 °C, and melt quenched film.

significant changes as indicated in Fig. 2(B). The maximum emission of the spincoated film is red-shifted by 50 nm from its solution phase fluorescence maximum. The emission spectra of the annealed films are further red-shifted and have a much broader bandwidth. It is believed that thermal annealing of a conjugated polymer film can provide the necessary energy to allow the individual polymer strand to explore configuration space so that they can reorganize themselves towards forming lower energy structure. The amount of intermolecular interactions of the polymers will increase as a result of ordered packing [20]. In the present case, thermal treatment of the spincoated oligomer films above its melting point and then annealing at 120 or 70 °C or quenching at room temperature leads to the formation of supramolecular packing and growth of polymeric lamellae with higher order, as indicated in Fig. 1.

Table 1
Optical properties of TMS-terminated OPE pentamer

Samples	UV λ_{max} (nm)	PL λ_{max} (nm)[a]
Solution	413	457 (486)
Spincoated film	425, 437, 461	(494) 508 (532)
Annealed film at 70 °C	436, 465	539
Annealed film at 120 °C	434, 462	539
Melt-quenched film	438, 466	550

[a] The values in parentheses refer to emission shoulders.

It is interesting to note that the PL spectra of films annealed at 70 and 120 °C have the same emission spectra centered at 539 nm, while the spectrum of film quenched at room temperature shows an even further red-shift maxima (550 nm). This behavior is probably due to the different intermolecular interactions formed when crystallizing at different temperatures. The degree of interchain interactions strongly depends on the film morphology [9,17]. When the melted pentamer molecules were quenched at room temperature abruptly, supramolecular packing formed very quickly, which did not allow the backbones and the side chains to reorganize to very homogenous packing. Some molecules may be more closely packed than those in films annealed at 70 and 120 °C, while the chains in the other areas are less closely packed. As a result, the PL spectrum of melt-quenched film is slightly red-shifted and broader than the other two thermally treated films.

In order to gain better understanding of the nature of the photoexcited state, we measured the time-resolved photoluminescence of dilute solution, spincoated and annealed films of the OPE pentamer at an excitation wavelength of 400 nm. Fig. 3 shows the PL decay profiles of solution, spincoated and annealed (at 120 °C) films of the pentamer samples detected at their corresponding emission maxima. The decay traces of the samples annealed at 70 °C and melt-quenched at room temperature are very much similar to that of the sample annealed at 120 °C. All the PL profiles are well fitted by single-exponential decay process:

$$A(t)=A_0\exp\left(\frac{-t}{\tau}\right)$$

where $A(t)$ is the PL intensity at t, A_0 is the initial intensity, and τ is the observed lifetime. The lifetime of OPE pentamer in THF is evaluated to be 0.45 ns and the decays are independent of wavelength. Since there are no intermolecular interactions in dilute solution, the luminescence is resulted from intrachain singlet exciton. The corresponding PL decay dynamics of the spincoated film of the oligomers can also be described as monoexponential, with a lifetime of 0.3 ns. The reduced

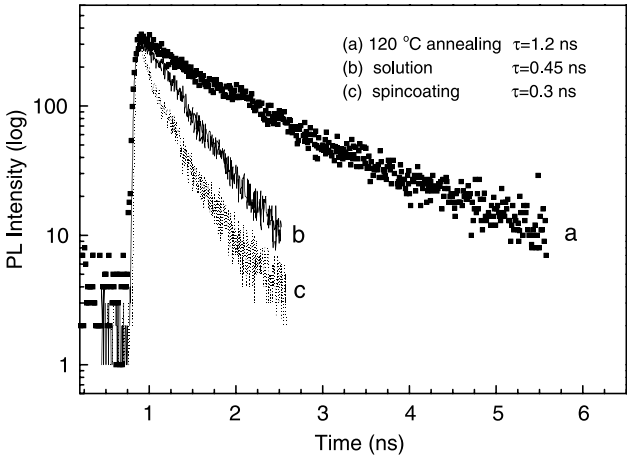

Fig. 3. PL decay profiles of OPE pentamer. Insert is the chemical structure of the oligomer.

lifetime for spincoated film is probably due to the increased non-radiative decay pathways, which include excitation energy transfer from singlet exciton to aggregates, excimers or defect traps. Upon annealing, the PL decays of the oligomer films change significantly compared with spincoated film. The lifetimes of melt-crystallized, 70 and 120 °C annealed films are 1.03, 0.94 and 1.2 ns, respectively. Longer luminescent lifetime in the annealed films and broader, structureless red-shifted emission spectra indicate again the existence of intermolecular excitation/emission. At present, we could not unambiguously assign the processes to aggregates but not excimers. It is most likely that excimers are also involved in the exciton relaxation. The longest lifetime observed in PL decay of the film annealed at 120 °C as well as the highest intensity of absorbance at low energy (from 500 to 650 nm in the absorption spectrum) imply that annealing at higher temperature will result in more ordered packing and higher degree of interchain interactions.

X-ray diffraction and molecular simulation are applied to obtain further information on the molecular packing of the spincoated and thermally treated films. The XRD patterns of the four films are shown in Fig. 4. The values of *d* spacings are summarized in Table 2. It can be found that the diffraction pattern of spincoated film (Fig. 4(a)) is very different from those of melt-crystallized film samples (Fig. 4(b)–(d)). These measurements indicated that the difference in film preparation conditions (spincoating or thermally annealing) will result in not only the difference in morphology (shown in Fig. 1) but also the difference in molecular packing in the crystals, which is directly associated with the optical properties of the films (shown in Figs. 2 and 3). The three melt-crystallized films show similar and distinct diffraction patterns at both the low-angle region and wide-angle region. The diffraction pattern of the film annealed at 120 °C, for example, shows prominent reflections at *d* spacing of 17.9, 15.9, 12.7 and 11.0 Å at low-angle region. The diffraction peaks at 17.9 and 15.9 Å are

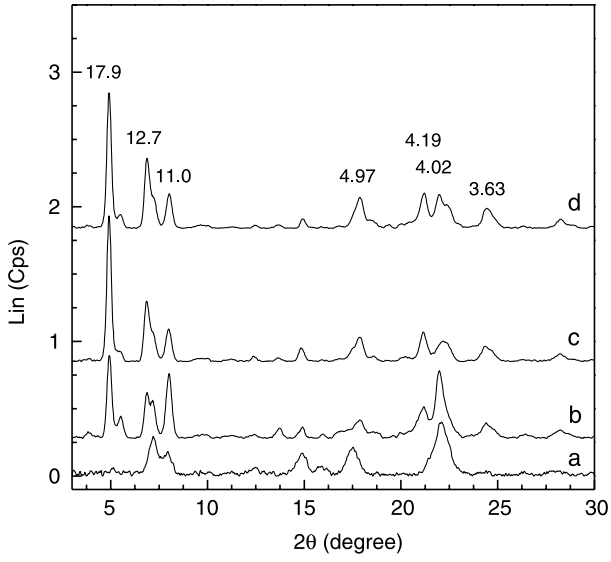

Fig. 4. X-ray diffraction patterns of films of spincoating (a), melt quenching (b), annealing at 70 °C (c), and annealing at 120 °C (d).

Table 2
XRD data (Å) of TMS-terminated OPE pentamer

Film	Low-angle region	Wide-angle region
Spincoating	12.2, 11.2	5.1, 4.0
Annealing at 70 °C	17.9, 15.9, 12.7, 11.0	5.0, 4.2, 4.0, 3.9, 3.6
Annealing at 120 °C	17.9, 15.9, 12.7, 11.0	5.0, 4.2, 3.6
Melt-quenching	17.9, 15.9, 12.7, 11.0	5.0, 4.2, 4.0, 3.6

indicative of a lamellar orientation of the side chains, which are not observed in spincoating films. The peaks at 12.7 and 11.0 Å are correlated to the interdigitated morphology [33]. Molecular simulation on the packing of pentamer molecules indicated two favorable models, which are end-to-end lamellar model and interdigitation model. The lateral distances between the backbones of two pentamer molecules in energy minimized lamellar and interdigitated conformations are 23.5 and 14 Å, respectively, which are larger than the data obtained from XRD measurement. Furthermore, molecular dynamics simulation shows that the distance between the two backbones ranges from 16 to 18 Å after the system reaching equilibrium in lamellar conformation. These data coincide well with the experimental results. The diffraction peaks at 3.6, 4.0, and 4.2 Å are assigned to the vertical distance between two oligomer backbones (90° angle). The distance is similar with the π-stacking distance of dialkyl and dialkoxy-substituted PPEs reported by Bunz [33] and Wrighton [34]. Our molecular simulation shows that the π-stacking distance is 3.7 Å and the conjugated backbones in the lamellar model display a staggered conformation between two main chains in both vertical and horizontal planes. The diffraction peak at 4.97 Å (d_1) exactly represents the distance of a phenyl ring in one chain to another phenyl ring on the adjacent chain in the vertical plane, which forms an angle of 43° with the vertical line (d_2 = 3.6 Å) between the two molecular main chains. This result is in good agreement with the calculated value (5.0 Å) for two diffracting planes involving two benzene rings, if the interchain spacing is 3.6 Å. The packing model is schematically shown in Chart 1.

Besides experimental characterization, we also performed molecular mechanics and molecular dynamics simulation using Cerius^2 software suite to model the molecular packing. For an isolated pentamer molecule in vacuum, the optimized typical geometric lengths of the planar extensive conformation are 42.5 Å for the end-to-end length of the conjugated backbone and 22 Å for the end-to-end length of side groups,

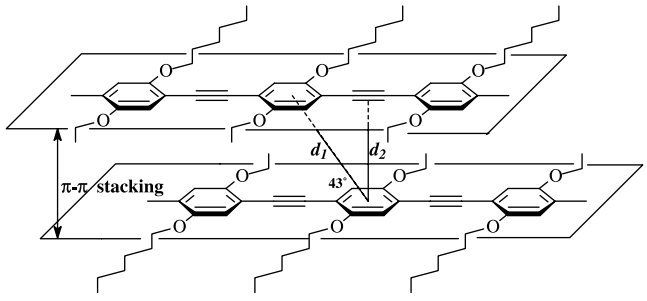

Chart 1. Schematic lamellar staggered conformation and distance.

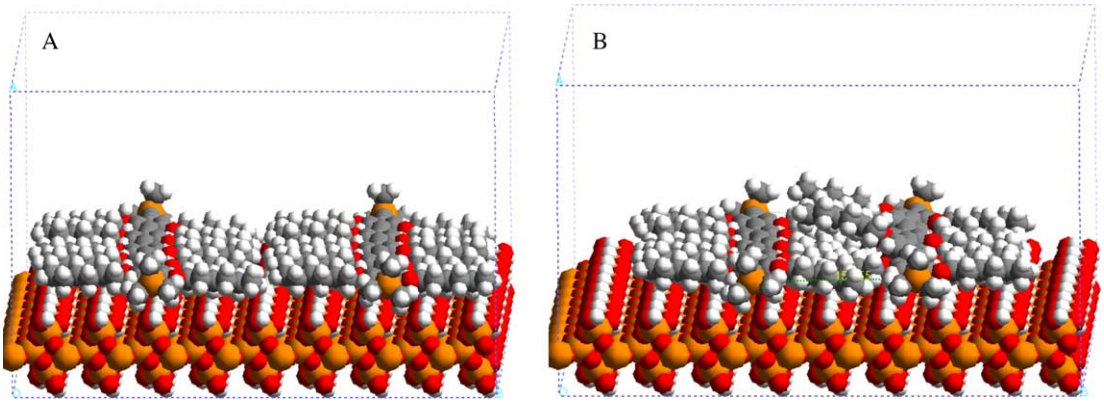

Fig. 5. Two OPE pentamer molecules on the hydrogenated quartz (100) surface, energy minimization conformations simulated by using molecular mechanics. Side-by-side, the lateral distance between the conjugated backbones is about (A) 23.5 Å , side view; (B) 14 Å (interdigitated), side view.

respectively. For two molecules in vacuum, the on-top stacking conformations are energetically more favorable than the side-by-side conformations, which are contributed to the strong attractive van der Waals interactions between the two molecules in the former conformation. The vertical distance between the conjugated backbones in the on-top stacking energy minimization conformation is 3.7 Å with the bulky trimethylsilyl terminals bending to the outer sides. A similar governing π–π stacking of the conjugated polymer chains has been pointed out by Leclere et al. when they studied the assembly of poly(*p*-phenyleneethynylene)-based block copolymers [35].

The interaction of the molecules with a quartz crystal substrate is simulated using molecular mechanics energy minimization and COMPASS force field. The unit cell of quartz (alpha) crystal is supplied in the Cerius^2 software database. The crystal is cleaved along the (100) face, which is predicted by Cerius^2—morphology as a dominant face of the crystal. A crystalline superlattice is built based on 9×9 of the cleaved (100) surface unit cell with a 20 Å of vacuum thickness. The surface is then hydrogenated before introducing the oligomer molecules onto it. To avoid having to use a very large slab as a substrate, periodic boundary conditions are implemented. All the atoms of the substrate are fixed during the MM/MD calculations. As the pentamer molecules are introduced onto the quartz surface (hydrogenated (100) surface), the molecules tend to lie planar on the surface with the backbone ring planes parallel to the surface. Fig. 5(A) and (B) shows the energy minimized conformations of two pentamer molecules lying side-by-side on the quartz surface with lateral distance of 23.5 Å (lamellar) and 14 Å (interdigitated) between the backbones and the binding energies between the molecule and the substrate are −97.47 and −87.59 kcal/mol for the lamellar and interdigitated conformations, respectively. The surface binding energy is the interaction energy between a molecule and a specific surface. The larger the absolute value of this negative number, the stronger the binding of the molecule to the crystal surface. Therefore, the lamellar assembly is more favorable. As the energy difference is not very obvious, there should be certain amount of interdigitated conformation in the films. The diffraction peaks at 12.7 and 11.0 Å support the existing of interdigitated conformation. However, due to the steric hindrance or interactions, some of the side groups could not be well packed as shown in Fig. 5(B). As the spacing between two side-by-side neighboring pentamer molecules decreases, their side groups stagger into each other.

A molecular dynamics simulation (NVT ensemble, the temperature maintained at 300 K, selecting Ewald method for Coulomb interaction and direct method for van der Waals interaction, other settings are set as default) is performed on the MM optimized structure in Fig. 5(B) as a starting conformation. A snapshot is shown in Fig. 6. As we can see, the side groups are flexible and irregular and some are protruding up. The distances between the two backbones at different positions along the backbone ranged from 10 to 20 Å and the same measurement fluctuated between 16 and 18 Å after the system reached equilibrium, which is in excellent agreement with experimental data from X-ray diffraction. The conjugated backbone end-to-end lengths change slightly because the backbone is very rigid. Upon addition of two more molecules

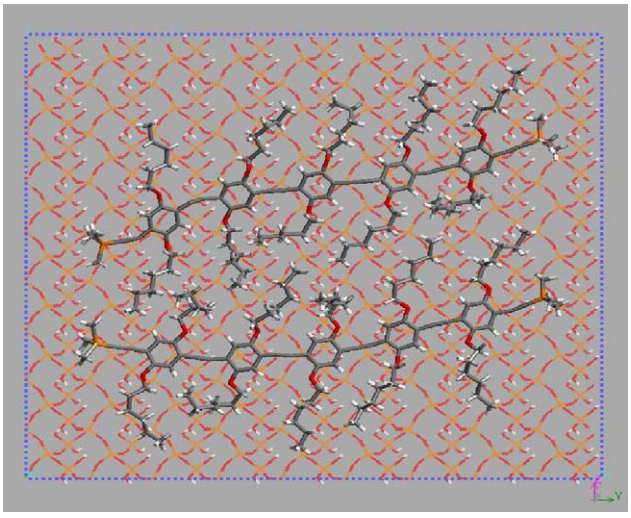

Fig. 6. A snapshot of molecular dynamics simulation for two TMS-terminated OPE pentamer molecules on quartz (100) surface at room temperature. The substrate is represented in stick for simplification and the molecules are represented in cylinder.

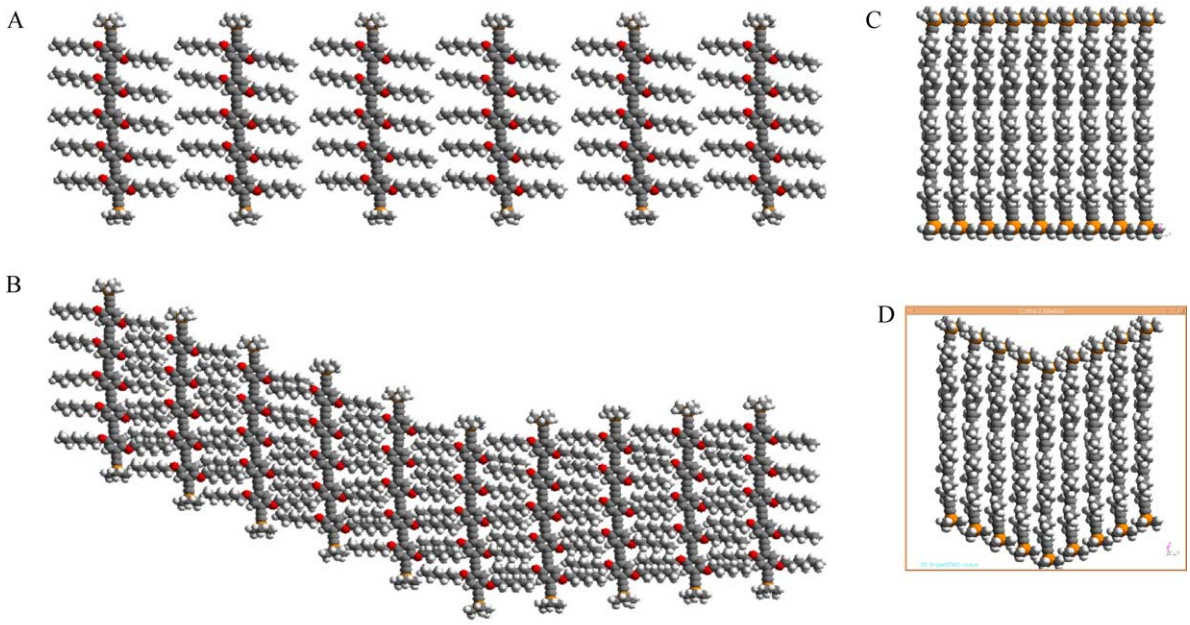

Fig. 7. Schematic models: (A) for lath and (B) for curved or bamboo morphology for OPE pentamer.

on-top of the conformation in Fig. 5(B), a similar MD simulation was performed. With two layers of molecules on-top of the quartz surface, we found that the molecular side chains at the bottom layer became more regular and their backbones became more planar.

On the basis of MM/MD simulation results, two models as illustrated in Fig. 7(A) and (B) were assumed for the molecular assembly on a quartz surface. Fig. 7(A) shows the most likely assembly near the surface, which could count for the formation of long straight laths; while occasionally, two differently oriented molecular blocks stagger together as shown in Fig. 7(B) and consequently form the curved sections or even joints. This may be the reason behind the observation of the unique 'bamboo' structure formed in the films annealed at 120 °C.

4. Conclusions

In summary, we have investigated the influence of thermal treatment on the morphologies and optical properties of phenyleneethynylene pentamer films. Thermal annealing was found to affect the morphologies of the oligomer films drastically. The homogeneous grainy morphology of the spincoated films reorganize into well-ordered single crystal-like lamellar laths or bamboo-like structures upon heating the films and then cooling to the designed temperature. The varied film morphologies lead to significant changes of their optical properties. Broader, red-shifted PL spectra and longer lifetime PL dynamics were observed in the annealed films, indicating the formation of lower energy structure (aggregates and excimers) due to strong interchain interaction. Thermal annealing to develop well-organized and closely packed films is a facile approach to achieve electronic or optoelectronic devices with optimized performance, e.g. thin film transistors with high charge carrier mobility.

References

[1] Burroughes JH, Bradley DDC, Brown AR, Marks RN, Mackay K, Friend RH, et al. Nature 1990;347:539.
[2] Friend RH, Gymer RW, Holmes AB, Burroughes JH, Marks RN, Taliani C, et al. Nature 1999;397:121.
[3] Katz HE, Bao ZN, Gilat SL. Acc Chem Res 2001;34:359.
[4] Brabec CJ, Cravino A, Meissner D, Sariciftci NS, Fromherz T, Rispens MT, et al. Adv Funct Mater 2001;1:374.
[5] McGehee MD, Heeger AJ. Adv Mater 2000;12:1655.
[6] Bumm LA, Arnold JJ, Cygan MT, Dunbar TD, Burgin TP, Jones II L, et al. Science 1996;271:1705.
[7] Joachim C, Gimzewski JK, Aviram A. Nature 2000;408:541.
[8] Dimitrakopoulos CD, Malenfant PRL. Adv Mater 2002;14:99.
[9] Nguyen T-Q, Kwong RC, Thompson ME, Schwartz BJ. Appl Phys Lett 2000;76:2454.
[10] Nguyen T-Q, Schwartz BJ, Schaller RD, Johnson JC, Lee LF, Haber LH, et al. J Phys Chem B 2001;105:5153.
[11] Lee TW, Park OO. Adv Mater 2000;12:801.
[12] Niu YH, Hou Q, Cao Y. Appl Phys Lett 2002;81:634.
[13] Shaheen SE, Brabec CJ, Sariciftci NS, Padinger F, Fromherz T, Hummelen JC. Appl Phys Lett 2001;78:841.
[14] Arias AC, MacKenzie JD, Stevenson R, Halls JJM, Inbasekaran M, Woo EP, et al. Macromolecules 2001;34:6005.
[15] Cadby AJ, Lane PA, Mellor H, Martin SJ, Grell M, Giebeler C, et al. Phys Rev B 2000;62:15604.
[16] Moons E. J Phys Condens Mater 2002;14:12235.
[17] Nguyen T-Q, Martini IB, Liu J, Schwartz BJ. J Phys Chem B 2000;104:237.
[18] Shi Y, Liu J, Yang Y. J Appl Phys 2000;87:4254.
[19] Tan CH, Inigo AR, Fann W, Wei P-K, Perng G-Y, Chen S-A. Org Electron 2002;3:81.
[20] Schaller RD, Snee PT, Johnson JC, Lee LF, Wilson KR, Haber LH, et al. J Chem Phys 2002;117:6688.
[21] Bunz UHF. Acc Chem Res 2001;34:998.
[22] Tour JM. Acc Chem Res 2000;33:791.

[23] Halkyard CE, Rampey ME, Kloppenburg L, Studer-Martinez SL, Bunz UHF. Macromolecules 1998;31:8655.
[24] Li H, Powell DR, Hayashi RK, West R. Macromolecules 1998;31:52.
[25] Deans R, Kim J, Machacek MR, Swager TM. J Am Chem Soc 2000;122: 8565.
[26] Zhou C-Z, Liu TX, Xu J-M, Chen Z-K. Macromolecules 2003;36:1457.
[27] Sun H. J Phys Chem B 1998;102:7338.
[28] Tanaka H, Gomez MA, Tonelli AE, Lovinger AJ, Davis DD, Thakur M. Macromolecules 1989;22:2427.
[29] Bout DAV, Kerimo J, Higgins DA, Barbara PF. Acc Chem Res 1997;30:204.
[30] Hosaka N, Tachibaba H, Shiga N, Matsumoto M, Tokura Y. Phys Rev Lett 1999;82:1672.
[31] Teetsov J, Fox MA. J Mater Chem 1999;9:2117.
[32] Huang WY, Matsuoka S, Kwei TK, Okamoto Y. Macromolecules 2001; 34:7166.
[33] Bunz UHF, Enkelmann V, Kloppenburg L, Jones D, Shimizu KD, Claridge JB, et al. Chem Mater 1999;11:1416.
[34] Weder C, Wrighton MS. Macromolecules 1996;29:5157.
[35] Leclere P, Hennebicq E, Calderone A, Brocorens P, Grimsdale AC, Müllen K, et al. Prog Polym Sci 2003;28:55.